Octadecanuclearity in Manganese Carboxylate Chemistry: Preparation and Properties of $K_4[Mn_{18}O_{16}(O_2CPh)_{22}(phth)_2(H_2O)_4]\cdot 10MeCN$

Rachel C. Squire,[†] Sheila M. J. Aubin,[‡] Kirsten Folting,[†] William E. Streib,[†] George Christou,*[,†] and David N. Hendrickson*[,‡]

Department of Chemistry and Molecular Structure Center, Indiana University, Bloomington, Indiana 47405-4001, and Department of Chemistry-0358, University of California at San Diego, La Jolla, California 92093-0358

Received February 24, 1995[⊗]

The synthesis and magnetochemical properties of $K_4[Mn_{18}O_{16}(O_2CPh)_{22}(phth)_2(H_2O)_4]\cdot 10MeCN$ (**5a**) are reported. This complex was prepared by the reaction of $(NBu^n_4)[Mn_4O_2(O_2CPh)_9(H_2O)]$ with potassium hydrogen phthalate, KH(phth). Complex **5a** crystallizes in monoclinic space group *C2/c* with the following cell parameters at −167 °C: $a = 22.673(5)$ Å, $b = 33.426(7)$ Å, $c = 27.991(8)$ Å, $\beta = 105.06(1)°$, $V = 20\,484$ Å^3, and $Z = 4$. The structure was refined employing 13 479 unique reflections with $F > 3\sigma(F)$ to give $R = 0.0607$ and $R_w = 0.0606$. Complex **5a** has eighteen Mn^{III} ions held together by sixteen μ_3-O^{2-} ions to give a $[Mn_{18}O_{16}]^{22+}$ core. The two phthalate ($phth^{2-}$) groups each bridge a total of four Mn atoms with each of their oxygen atoms terminally ligated. The $[Mn_{18}O_{16}]^{22+}$ core can be described as arising from the fusion of five $[Mn_4(\mu_3\text{-}O)_2]^{8+}$ units possessing either a planar or bent ("butterfly") Mn_4 unit. Three such units are fused body-to-body to give the central $[Mn_{10}O_6]^{18+}$ unit. Two additional $[Mn_4O_2]^{8+}$ units are attached to the $[Mn_{10}O_6]^{18+}$ unit at the six "wing-tip" positions. Variable-temperature and variable-field dc magnetic susceptibility data were collected for a polycrystalline sample of the MeCN-desolvated complex **5**. In a 10.0 kG field μ_{eff} per molecule varies gradually from 15.1 μ_B at 320 K to 1.73 μ_B at 2.00 K. Alternating current (ac) magnetic susceptibility data measured in the 2.0−60.0 K range in zero dc field with a 1.0 G ac field oscillating at 50 Hz nearly superimpose with the dc susceptibility data. As the temperature approaches zero, $\chi_M T$ approaches zero. Thus, the Mn^{III}_{18} complex **5** has a $S = 0$ ground state. This is unusual for polynuclear Mn^{III} complexes, which generally have high-spin ground states. The $S = 0$ ground state for complex **5** is explained in terms of spin frustration that is likely present in the $[Mn_4O_2]^{8+}$ butterfly building blocks.

Introduction

Fascination with polynuclear coordination complexes has existed for at least 150 years. Polynuclear cobalt(III) ammine complexes were first prepared as long ago as 1852, when Fremy[1] synthesized the diamagnetic (μ-peroxo)decaamminedicobalt(III) ion by oxidizing an ammoniacal Co^{II} solution with air. There is a growing list[2] of proteins and enzymes that are known to have active sites comprised of polynuclear metal complexes. The nuclearities of these active sites range from 2 to ~4500. There has been considerable effort expended in order to prepare complexes that model the active sites. During the course of these studies, serendipity has occasionally come into play. A ligand may be designed to give a dinuclear complex for example, but a higher nuclearity complex may instead result when the ligand reacts with metal ions in solution. This serendipity has recently led to several interesting polynuclear iron and manganese complexes.

Polynuclear iron complexes are being studied for at least two different reasons.[3] First, it is important to understand the iron storage protein ferritin,[4] which is involved in the storage, detoxification, and recycling of iron. Ferritin can store up to ~4500 ferric ions in its protein core. Second, larger and larger polynuclear iron complexes are being studied to understand the factors controlling when a complex becomes large enough to exhibit properties of single-domain iron oxide particles. Recently, Taft *et al.*[5] and Papaefthymiou[6] employed Mössbauer spectroscopy to demonstrate the presence of superparamagnetism in Fe_{12} and $Fe_{16}M$ molecular complexes. As a result of the intrinsic nature of various ligands and through controlled polymerization of iron ions in nonaqueous media, complexes of Fe_4,[7] Fe_6,[8] Fe_8,[9,10] Fe_{10},[11,12] Fe_{11},[13] Fe_{12},[5,6] $Fe_{16}M$,[15] Fe_{17},[16]

[†] Indiana University.
[‡] University of California at San Diego.
[⊗] Abstract published in *Advance ACS Abstracts,* November 1, 1995.

(1) (a) Fremy, E. *Ann. Chim. Phys.* **1852**, *35*, 257. (b) Fremy, E. *Ann. Chim. Phys.* **1852**, *83*, 289.
(2) (a) *Principles of Bioinorganic Chemistry*; Lippard, S. J., Berg, J. M., Eds.; University Science Books: Mill Valley, CA, 1994. (b) *Inorganic Biochemistry, An Introduction*; Cowan, J. A., Ed.; VCH Publishers: New York, 1993.
(3) (a) Lippard, S. J. *Angew. Chem., Int. Ed. Engl.* **1988**, *27*, 344. (b) Hagen, K. S. *Angew. Chem., Int. Ed. Engl.* **1992**, *31*, 1010. (c) Powell, A. K.; Heath, S. L. *Comments Inorg. Chem.* **1994**, *15*, 255. (d) Gatteschi, D.; Caneschi, A.; Pardi, L.; Sessoli, R. *Science* **1994**, *265*, 1054.
(4) (a) Theil, E. C. *Annu. Rev. Biochem.* **1987**, *56*, 289, and references cited therein. (b) Xu, B.; Chasteen, D. *J. Biol. Chem.* **1991**, *266*, 19965.
(5) (a) Taft, K. L.; Papaefthymiou, G. C.; Lippard, S. J. *Science* **1993**, *259*, 1302. (b) Taft, K. L.; Papaefthymiou, G. C.; Lippard, S. J. *Inorg. Chem.* **1994**, *33*, 1510.
(6) Papaefthymiou, G. C. *Phys. Rev.* **1992**, *B46*, 10366.
(7) (a) McCusker, J. K.; Vincent, J. B.; Schmitt, E. A.; Mino, M. L.; Shin, K.; Coggin, D. K.; Hagen, P. M.; Huffman, J. C.; Christou, G.; Hendrickson, D. N. *J. Am. Chem. Soc.* **1991**, *113*, 3012, and references cited therein. (b) Gorun, S. M.; Lippard, S. J. *Inorg. Chem.* **1988**, *27*, 149. (c) Murch, B. P.; Bradley, F. C.; Boyle, P. D.; Papaefthymiou, V.; Que, L., Jr. *J. Am. Chem. Soc.* **1987**, *109*, 7993. (d) Armstrong, W. H.; Roth, M. E.; Lippard, S. J. *J. Am. Chem. Soc.* **1987**, *109*, 6318.
(8) (a) Christmas, C. A.; Tsai, H.-L.; Pardi, L.; Kesselman, J. M.; Gantzel, P. K.; Chadha, R. K.; Gatteschi, D.; Harvey, D. F.; Hendrickson, D. N. *J. Am. Chem. Soc.* **1993**, *155*, 12483, and references cited therein. (b) Nair, V. S.; Hagen, K. S. *Inorg. Chem.* **1992**, *31*, 4048. (c) Harding, C. J.; Henderson, R. K.; Powell, A. K. *Angew. Chem., Int. Ed. Engl.* **1993**, *32*, 570.

0020-1669/95/1334-6463$09.00/0

and Fe_{19}[5,6] have been reported. Oxide, hydroxide, and carboxylate anions usually serve as the bridges between the iron ions.

The pursuit of effective models for the active sites of the water oxidation center of photosystem II and manganese catalases has also led to polynuclear manganese complexes. For the most part the use of relatively simple ligands has led to the characterization of, for example, Mn_4,[17] Mn_7,[18,19] Mn_8,[20] Mn_9,[20ab,21] Mn_{10},[22] Mn_{11},[23] Mn_{12},[24-27] and Mn_{16}[28,29] complexes. Oxide and carboxylate anions also serve as the bridges in these complexes. The structures of many of these complexes can be envisioned as being made up of μ_3-oxo-bridged Mn_3 triangles or $Mn_4(\mu_3\text{-}O^{2-})_2$ butterfly units.

In contrast to the Fe_x complexes that frequently have low-spin (*i.e.*, $S = 0$ or $S = {}^1/_2$) ground states, several of the Mn_x complexes have relatively high-spin ground states: $Mn^{IV}Mn^{III}_3$ complexes[17f,g] with $S = {}^9/_2$ ground states, a Mn^{III}_7 complex[18] with $S = 3$, and $Mn^{IV}_4Mn^{III}_8$ complexes[24b,26] with $S = 9$ or 10 ground states. The pairwise Mn···Mn exchange interactions are mostly antiferromagnetic; "spin frustration"[30] is the origin of the relatively high-spin ground states. Certain topological arrangements of Mn^{III} ions not only lead to spin frustration and resultant high-spin ground states, but there can also be appreciable zero-field splitting in the ground states. Each Mn^{III} ion is Jahn-Teller distorted and has a significant single-ion zero-field splitting. If the distortion axes of Mn^{III} ions in a complex are close to parallel, then the single-ion zero-field interactions will lead to appreciable zero-field splitting in the ground state.

The three Mn_{12} complexes of composition $[Mn_{12}O_{12}(O_2CR)_{16}(H_2O)_4]$ [R = Me (**1**),[24,25] Et (**2**),[26] or Ph (**3**)[24b]] and the one-electron reduction product $(PPh_4)[Mn_{12}O_{12}(O_2CEt)_{16}(H_2O)_4]$ (**4**)[26] are not only some of the highest nuclearity manganese complexes known, but they exhibit unusual magnetic susceptibility relaxation effects. At low-temperatures an out-of-phase alternating current (ac) susceptibility signal is seen for these four complexes. The magnetization of each Mn_{12} complex cannot stay in phase with the oscillating magnetic field in the ac susceptibility experiment. Each Mn_{12} complex is functioning as a magnetizable magnet. Well-developed hysteresis loops can be seen for the four complexes. These are the only molecular species known to exhibit this property. Zero-field splitting in the high-spin ground state leads to appreciable magnetic anisotropy and, consequently, to the relaxation effects. There is considerable theoretical interest[31,32] in various aspects of these "nanoscale" magnets.

The unusual properties of the above Mn_{12} complexes make it desirable to prepare and characterize Mn_x complexes with nuclearities greater than 12. In this paper we report the preparation of a Mn^{III}_{18} complex, $K_4[Mn_{18}O_{16}(O_2CPh)_{22}(phth)_2(H_2O)_4]$ (**5**) where $phthH_2$ is phthalic acid. This represents a significant increase in the nuclearity of manganese complexes.

Experimental Section

Synthesis. All manipulations were performed under aerobic conditions using materials as received. The complex $(NBu^n_4)[Mn_4O_2(O_2CPh)_9(H_2O)]$ (**6**) was prepared as described elsewhere.[33]

$K_4[Mn_{18}O_{16}(O_2CPh)_{22}(phth)_2(H_2O)_4]\cdot 10MeCN$ (5a). To a stirred, red-brown solution of complex **6** (0.25 g, 0.16 mmol) in MeCN (50 mL) was added solid potassium hydrogen phthalate (0.033 g, 0.16 mmol) in small portions. The slurry was stirred for 5 days and then filtered to remove an off-white powder. The red-brown filtrate was allowed to slowly concentrate by evaporation at ambient temperature over 10 days, and the resultant essentially black crystals were collected by filtration, washed with hexanes, and dried *in vacuo*. The yield was ~30% based on Mn. Additional crystals (~10% yield) can be obtained from the filtrate on further concentration for 1-2 weeks, for a combined yield of ~40%. A sample kept in contact with the mother liquor was identified crystallographically as the title compound (**5a**); drying under vacuum gives the MeCN-free form. Anal. Calcd (found) for $C_{170}H_{126}O_{72}K_4Mn_{18}$: C, 45.72 (45.50); H, 2.84 (2.80); K, 3.49 (3.50); Mn, 22.14 (21.98). Selected IR data (KBr, cm^{-1}): 3422 (br, w), 1597

(9) (a) Wieghardt, K.; Pohl, K.; Jibril, I.; Huttner, G. *Angew. Chem., Int. Ed. Engl.* **1984**, *23*, 77. (b) Delfs, C.; Gatteschi, D.; Pardi, L.; Sessoli, R.; Wieghardt, K.; Hanke, D. *Inorg. Chem.* **1993**, *32*, 3099.
(10) Nair, V. S.; Hagen, K. S. *Inorg. Chem.* **1994**, *33*, 185.
(11) Taft, K. L.; Lippard, S. J. *J. Am. Chem. Soc.* **1990**, *112*, 9629.
(12) Taft, K. L.; Delfs, C. D.; Papaefthymiou, G. C.; Foner, S.; Gatteschi, D.; Lippard, S. J. *J. Am. Chem. Soc.* **1994**, *116*, 823.
(13) Gorun, S. M.; Papaefthymiou, G. C.; Frankel, R. B.; Lippard, S. J. *J. Am. Chem. Soc.* **1987**, *109*, 3337.
(14) Micklitz, W.; McKee, V.; Rardin, R. L.; Pence, L. E.; Papaefthymiou, G. C.; Bott, S. G.; Lippard, S. J. *J. Am. Chem. Soc.* **1994**, *116*, 8061.
(15) Powell, A. K.; Heath, S. L. *J. Am. Chem. Soc.* **1995**, *117*, 2491.
(16) Heath, S. L.; Powell, A. K. *Angew. Chem., Int. Ed. Engl.* **1992**, *31*, 191.
(17) (a) Vincent, J. B.; Christmas, C.; Chang, H.-R.; Li, Q.; Boyd, P. D. W.; Huffman, J. C.; Hendrickson, D. N.; Christou, G. *J. Am. Chem. Soc.* **1989**, *111*, 2086. (b) Wang, S.; Folting, K.; Streib, W. E.; Schmitt, E. A.; McCusker, J. K.; Hendrickson, D. N.; Christou, G. *Angew. Chem., Int. Ed. Engl.* **1991**, *30*, 304. (c) Libby, E.; McCusker, J. K.; Schmitt, E. A.; Folting, K.; Hendrickson, D. N.; Christou, G. *Inorg. Chem.* **1991**, *30*, 3486. (d) Bouwman, E.; Bolcar, M. A.; Libby, E.; Huffman, J. C.; Folting, K.; Christou, G. *Inorg. Chem.* **1992**, *31*, 5185. (e) Hendrickson, D. N.; Christou, G.; Schmitt, E. A.; Libby, E.; Bashkin, J. S.; Wang, S.; Tsai, H.-L.; Vincent, J. B.; Boyd, P. D. W.; Huffman, J. C.; Folting, K.; Li, Q.; Streib, W. E. *J. Am. Chem. Soc.* **1992**, *114*, 2455. (f) Schmitt, E. A.; Noodleman, L.; Baerends, E. J.; Hendrickson, D. N. *J. Am. Chem. Soc.* **1992**, *114*, 6109.
(18) Wang, S.; Tsai, H.-L.; Streib, W. E.; Christou, G.; Hendrickson, D. N. *J. Chem. Soc., Chem. Commun.* **1992**, 667.
(19) Bhula, R.; Weatherburn, D. C. *Angew. Chem., Int. Ed. Engl.* **1991**, *30*, 688.
(20) (a) Wang, S.; Huffman, J. C.; Folting, K.; Streib, W. E.; Lobkovsky, E.; Christou, G. *Angew. Chem., Int. Ed. Engl.* **1991**, *30*, 1672. (b) Tsai, H.-L.; Wang, S.; Folting, K.; Streib, W. E.; Hendrickson, D. N.; Christou, G. *J. Am. Chem. Soc.* **1995**, *117*, 2503. (c) Libby, E.; Folting, K.; Huffman, C. J.; Huffman, J. C.; Christou, G. *Inorg. Chem.* **1993**, *32*, 2549. (d) Wang, S.; Tsai, H.-L.; Folting, K.; Martin, J. D.; Hendrickson, D. N.; Christou, G. *J. Chem. Soc., Chem. Commun.* **1994**, 671. (e) Wemple, M. W.; Tsai, H.-L.; Streib, W. E.; Hendrickson, D. N.; Christou, G. *J. Chem. Soc., Chem. Commun.* **1994**, 1031.
(21) Christmas, C.; Vincent, J. B.; Chang, H.-R.; Huffman, J. C.; Christou, G.; Hendrickson, D. N. *J. Am. Chem. Soc.* **1988**, *110*, 823.
(22) (a) Eppley, H. J.; Aubin, S. M.; Hendrickson, D. N.; Christou, G. Manuscript in preparation. (b) Hagen, K. S.; Armstrong, W. M.; Olmstead, M. M. *J. Am. Chem. Soc.* **1989**, *111*, 774. (c) Goldberg, D. P.; Caneschi, A.; Delfs, C. D.; Sessoli, R.; Lippard, S. J. *J. Am. Chem. Soc.* **1995**, *117*, 5789. (d) Cavaluzzo, M.; Chen, Q.; Zubieta, J. *J. Chem. Soc., Chem. Commun.* **1993**, 131.
(23) Perlepes, S. P.; Huffman, J. C.; Christou, G. *J. Chem. Soc., Chem. Commun.* **1991**, 1657.
(24) (a) Lis, T. *Acta Crystallogr.* **1980**, *B36*, 2042. (b) Sessoli, R.; Tsai, H.-L.; Schake, A. R.; Wang, S.; Vincent, J. B.; Folting, K.; Gatteschi, D.; Christou, G.; Hendrickson, D. N. *J. Am. Chem. Soc.* **1993**, *115*, 1804.
(25) Caneschi, A.; Gatteschi, D.; Sessoli, R.; Barra, A. L.; Brunel, L. C.; Guillot, M. *J. Am. Chem. Soc.* **1991**, *113*, 5873.
(26) Eppley, H. J.; Tsai, H.-L.; de Vries, N.; Folting, K.; Christou, G.; Hendrickson, D. N. *J. Am. Chem. Soc.* **1995**, *117*, 301.
(27) Luneau, D.; Savariault, J.-M.; Tuchagues, J.-P. *Inorg. Chem.* **1988**, *27*, 3912.
(28) Gorun, S. M.; Stibrany, R. T. U. S. Patent 5,041,575, 1991.
(29) Gorun, S. M.; Stibrany, R. T.; Goshorn, D. P.; George, G. N. Abstract no. 234, Inorganic Chemistry Division, 207th ACS National Meeting, March 13-17, 1994.
(30) Hendrickson, D. N. In *Research Frontiers in Magnetochemistry*; O'Connor, C. J., Ed.; World Scientific Publishing Co.: Singapore, 1993; pp 87-108.
(31) Villain, J.; Hartman-Boutron, F.; Sessoli, R.; Rettori, A. *Europhys. Lett.* **1994**, *27*, 159.
(32) Loss, D.; Di Vincenzo, D. P.; Grinstein, G.; Awschalom, D. D.; Smyth, J. F. *Physica B* **1993**, *189*, 189.
(33) Wang, S.; Huffman, J. C.; Folting, K.; Streib, W. E.; Lobkovsky, E. B.; Christou, G. *Angew. Chem., Int. Ed. Engl.* **1991**, *30*, 1672.

Table 1. Crystallographic Data for $K_4[Mn_{18}O_{16}(O_2CPh)_{22}(phth)_2(H_2O)_4]\cdot 10MeCN$ (**5a**)

$C_{190}H_{156}N_{10}O_{72}K_4Mn_{18}$[a]	$Z = 4$
fw = 4876.72	$T = -167$ °C
space group *C2/c*	$\lambda = 0.710\ 69$ Å[b]
$a = 22.673(5)$ Å	$\rho_{calcd} = 1.58$ g cm^{-3}
$b = 33.426(7)$ Å	$\mu = 11.876$ cm^{-1}
$c = 27.991(8)$ Å	R[c] = 0.0607
$\beta = 105.06(1)°$	R_w[c] = 0.0606
$V = 20{,}484$ Å^3	

[a] Including solvate molecules. [b] Graphite monochromator. [c] $R = \sum||F_o| - |F_c||/\sum|F_o|$ and $R_w = [\sum w(|F_o| - |F_c|)^2/\sum w|F_o|^2]^{1/2}$, where $w = 1/\sigma^2|F_o|$.

(m), 1554 (m), 1520 (s), 1491 (m), 1448 (m), 1400 (vs), 1176 (m), 1068 (m), 1026 (m), 717 (s), 688 (m), 679 (m), 638 (m), 607 (m), 465 (m).

X-ray Crystallography. Data were collected on a crystal of complex **5a** using a Picker four-circle diffractometer; details of the diffractometry, low-temperature facilities and computational procedures employed by the Molecular Structure Center are available elsewhere.[34]

A single, dark-purple crystal was selected from the bulk sample, attached to a glass fiber using silicone grease, and transferred to the goniostat, where it was cooled to −167 °C for characterization and data collection. A systematic search of selected ranges of reciprocal space yielded a set of reflections that exhibited 2/*m* diffraction symmetry and *C*-centering (*hkl* extinct for $h + k, = 2n + 1$). Following complete data collection, the systematic extinction of 001 for $l = 2n + 1$ and of 0*k*0 for $k = 2n + 1$ limited the choice of possible space groups to *C2/c* (No. 15) or *Cc* (No. 9); subsequent structure solution and refinement confirmed the correct space group as *C2/c*. A total of 15 132 reflections (including standards and some space group extinctions) was collected. Data processing gave a unique set of 13 479 reflections and a residual of 0.073 for the averaging of 1149 reflections measured more than once. Plots of four standard reflections measured every 300 reflections showed no significant trends. An absorption correction was not performed. The structure was solved using MULTAN-78 and standard Fourier techniques. The non-hydrogen atoms were readily located, and many of the hydrogen atoms were evident in a subsequent difference Fourier map; three H atoms associated with the two unique water molecules were located [H(61), H(62), and H(63)], and the fourth H atom [H(64)] was introduced in a fixed calculated position, as were all of the H atoms on the phenyl rings. Full matrix, least-squares refinement was completed using anisotropic thermal parameters on all of the non-hydrogen atoms in the molecule of interest and isotropic thermal parameters on the solvent atoms. The asymmetric unit contains half of the Mn_{18} complex, two K cations as well as five molecules of solvent acetonitrile [N(139) through C(155)]. One of the solvent molecules is disordered [N(151) through C(155)]. The final $R(F)$ was 0.061 using the full unique data. Reflections having $F < 3.0\sigma(F)$ were given zero weight. Owing to the large number of atoms, the refinement was carried out in a cyclical manner. The total number of parameters varied was 1349, including the scale factor and an overall isotropic extinction parameter. The final difference map was essentially featureless, the largest peak being 0.78 e/Å^3 in the vicinity of C(144) in a solvent molecule, and the deepest hole being −0.75 e/Å^3. Final R and R_w values are listed in Table 1.

Physical Measurements. Infrared and electronic absorption spectra were recorded on Nicolet 510P FT-IR and Hewlett-Packard 8452A instruments, respectively. IR spectra were recorded on KBr pellets.

Direct current (dc) magnetic susceptibility measurements were carried out on a Quantum Design MPMS5 SQUID susceptometer equipped with a 55 kG magnet and operating in the range of 1.8−400 K. The temperature calibration accuracy is ±0.5% on a MPMS SQUID; the temperature stability is 0.05 K at 300 K and 0.01 K at 5.0 K. The stability in the magnetic field is 1 ppm/h. Alternating current (ac) magnetic susceptibility measurements were carried out on a Quantum Design MPMS2 SQUID ac susceptometer. The ac frequency range is

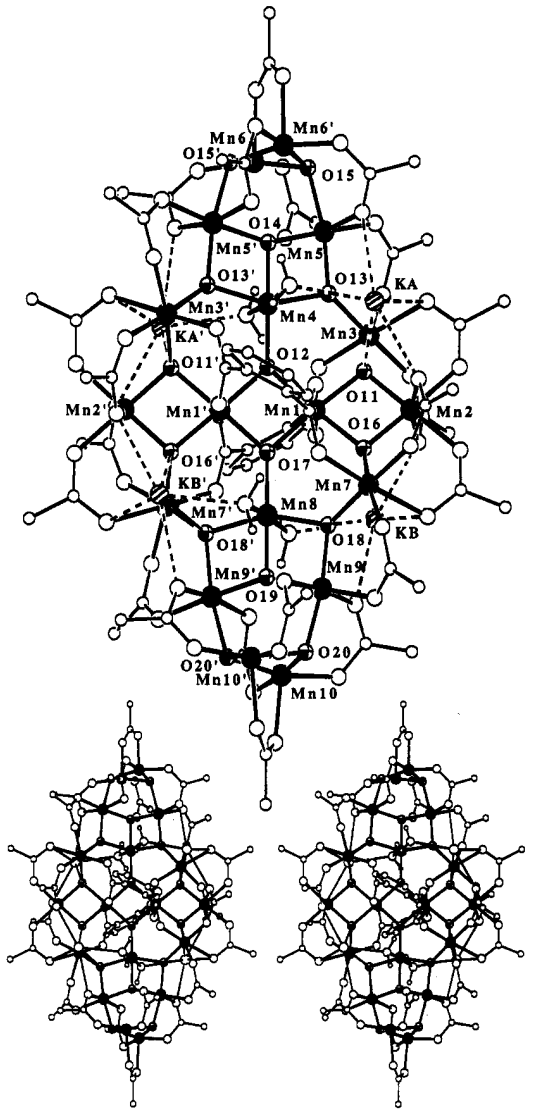

Figure 1. ORTEP representation and stereoview of $K_4[Mn_{18}O_{16}(O_2CPh)_{22}(phth)_2(H_2O)_4]$. All but one of the benzoate phenyl C atoms have been omitted for clarity. The terminal MeCN groups on the K^+ ions (KA and KB, diagonally shaded) are also omitted.

5.0×10^{-4} to 1.5 kHz, and the ac field strength can be varied from 10^{-4} to 5.0 G. Pascal's constants[35] were used to estimate the diamagnetic corrections for each complex, which were subtracted from the experimental susceptibilities to give the molecular paramagnetic susceptibilities.

Results and Discussion

Synthesis. The present work represents the latest stage of a continuing program concerned with developing synthetic methodologies to high-nuclearity Mn_x ($x \geq 6$) aggregates, and it takes advantage of the observation that the tetranuclear complexes containing the $[Mn_4(\mu_3\text{-}O)_2]^{8+}$ core are excellent springboards to a variety of such products. Thus, for example, $[Mn_4O_2(O_2CMe)_7(bpy)_2]^+$ (bpy = 2,2′-bipyridine) is converted to $[Mn_{11}O_{10}Cl_2(O_2CMe)_{11}(bpy)_2(MeCN)_2(H_2O)]$ with Me_3SiCl,[23] whereas $[Mn_4O_2(O_2CMe)_7(pic)_2]^-$ (picH = picolinic acid) is converted to $[Mn_8O_4(O_2CMe)_{12}(pic)_4]$ under these conditions.[20c]

(34) Chisholm, M. H.; Folting, K.; Huffman, J. C.; Kirkpatrick, C. C. *Inorg. Chem.* **1984**, *23*, 1021.

(35) *Theory and Applications of Molecular Paramagnetism*; Boudreaux, E. A., Mulay, L. N., Eds.; John Wiley & Sons: New York, 1976.

Table 2. Selected Fractional Coordinate ($\times 10^4$)[a] and Equivalent Isotropic Thermal Parameters ($\times 10$)[b] for $K_4[Mn_{18}O_{16}(O_2CPh)_{22}(phth)_2(H_2O)_4]\cdot 10MeCN$ (**5a**)

atom	x	y	z	B_{eq}, Å^2	atom	x	y	z	B_{eq}, Å^2
Mn(1)	5513.1(4)	1592.8(3)	7284.9(4)	11	O(51)	7042(2)	395(1)	7942(2)	19
Mn(2)	6550.4(5)	1592.0(3)	6855.9(4)	15	C(52)	7095(3)	32(2)	7828(2)	19
Mn(3)	6544.8(4)	831.6(3)	7583.0(4)	14	O(53)	6649(2)	−185(1)	7609(2)	21
Mn(4)	5000*	646.0(4)	7500*	11	O(60)	5666(2)	−107(1)	6667(2)	21
Mn(5)	5783.2(5)	−44.3(3)	7465.2(4)	16	C(61)	4447(4)	−415(2)	8599(3)	23
Mn(6)	5208(1)	−707.2(3)	8005.4(4)	22	O(62)	4844(3)	−676(1)	8555(2)	25
Mn(7)	5639.5(5)	2358.9(3)	6503.4(4)	15	O(69)	5958(2)	−112(1)	8345(2)	23
Mn(8)	5000*	2535.6(4)	7500*	14	C(70)	6245(4)	−416(2)	8559(3)	24
Mn(9)	5423(1)	3229.4(3)	7042.9(4)	19	O(71)	6019(3)	−765(2)	8476(2)	29
Mn(10)	5534(1)	3891.3(3)	7875.5(4)	26	O(78)	5153(3)	−1329(1)	7916(2)	34
O(11)	6116(2)	1231(1)	7154(2)	15	C(79)	5000*	−1502(3)	7500*	28
O(12)	5000*	1210(2)	7500*	11	O(84)	7002(2)	1969(1)	6540(2)	20
O(13)	5829(2)	517(1)	7434(2)	14	C(85)	6950(3)	2340(2)	6464(3)	22
O(14)	5000*	93(2)	7500*	15	O(86)	6612(2)	2573(1)	6633(2)	22
O(15)	5539(2)	−602(1)	7460(2)	20	O(93)	6029(2)	1441(1)	6104(2)	18
O(16)	5967(2)	1953(1)	6977(2)	14	C(94)	5870(3)	1724(2)	5792(3)	18
O(17)	5000*	1972(2)	7500*	13	O(95)	5757(2)	2078(1)	5916(2)	18
O(18)	5483(2)	2661(1)	7012(2)	17	O(102)	5446(2)	2807(1)	6027(2)	18
O(19)	5000*	3090(2)	7500*	19	C(103)	5605(3)	3169(2)	6071(3)	21
O(20)	5310(2)	3784(1)	7189(2)	22	O(104)	5713(2)	3370(1)	6469(2)	24
O(21)	6181(2)	1682(1)	8064(2)	17	O(111)	6322(2)	3262(1)	7532(2)	24
C(22)	6341(3)	1404(2)	8369(3)	16	C(112)	6623(4)	3570(2)	7707(3)	31
O(23)	6387(2)	1038(1)	8259(2)	16	O(113)	6403(3)	3854(2)	7917(2)	30
C(24)	6486(3)	1494(2)	8908(3)	16	O(120)	4426(3)	3287(1)	6509(2)	28
C(25)	7036(3)	1389(2)	9227(3)	20	C(121)	5746(4)	3583(2)	8779(3)	26
C(26)	7162(3)	1484(2)	9731(3)	22	O(122)	5740(3)	3934(1)	8601(2)	29
C(27)	3283(4)	1683(2)	5093(3)	23	O(129)	5409(3)	4507(1)	7829(2)	37
C(28)	3828(3)	1794(2)	5411(3)	17	C(130)	5000*	4676(3)	7500*	31
C(29)	3958(3)	1689(2)	5911(3)	15	O(135)	5396(2)	610(1)	8346(2)	16
C(30)	4568(3)	1784(2)	6257(2)	14	O(136)	5863(2)	2567(1)	8146(2)	18
O(31)	4861(2)	1505(1)	6498(2)	13	K(137)	5597(1)	736.8(5)	6359(1)	18
O(32)	4726(1)	2150(1)	6278(2)	16	K(138)	6694(1)	2463.6(5)	7646(1)	22
O(33)	7133(2)	1194(1)	6714(2)	22	N(142)	5455(3)	429(2)	5405(3)	33
C(34)	7146(3)	811(2)	6731(3)	21	C(143)	5582(4)	325(2)	5055(3)	26
O(35)	6843(2)	597(1)	6938(2)	19	C(144)	5747(4)	188(3)	4603(3)	32
O(42)	7240(2)	1755(1)	7547(2)	20	N(145)	7502(4)	2758(3)	8502(3)	57
C(43)	7524(3)	1476(2)	7799(3)	23	C(146)	7415(4)	2650(3)	8865(3)	39
O(44)	7330(2)	1119(1)	7802(2)	19	C(147)	7327(5)	2514(3)	9329(4)	50

[a] Parameters marked with an asterisk were fixed by symmetry. [b] $B_{eq} = {}^4/_3\sum\sum B_{ij}a_ia_j$.

Of particular relevance to the present work are the related reactions of $(NBu_4)[Mn_4O_2(O_2CPh)_9(H_2O)]$ (**6**),[33] the anion of which contains only $PhCO_2^-$ and H_2O peripheral ligation and is thus especially useful for synthesizing higher nuclearity products: it has, for example, permitted attainment of $[Mn_9Na_2O_7(O_2CPh)_{15}(MeCN)_2]$,[33] $(NBu^n_4)[Mn_8O_6Cl_6(O_2CPh)_7(H_2O)_2]$,[33] and $(NBu^n_4)_2[Mn_8O_4(O_2CPh)_{12}(Et_2mal)_2(H_2O)_2]$[20e] ($Et_2malH_2$ = 2,2-diethylmalonic acid) when treated with $(PhCO_2)_2$, Me_3SiCl, and $Na_2(Et_2mal)$, respectively. The latter reaction represented our first successful foray into dicarboxylate chemistry, and the present work is an extension of this effort to phthalic acid. Within Mn chemistry, this dicarboxylic acid has been little employed, although it has been shown to give $[Mn_4(phth)_2(bpy)_4]^{4+}$ with Mn^{II} sources.[36]

Treatment of complex **6** with 1 equiv of potassium hydrogen phthalate, KH(phth), in MeCN gave no noticeable color change but subsequently resulted in slow crystallization of **5a**, which is converted to the MeCN-free form (**5**) on drying *in vacuo*. The yields of pure material (~40%) are sufficient for subsequent study. The addition of NR_4^+ (R = alkyl) or PPh_4^+ salts to the reaction filtrate gave precipitates of material whose IR spectra and elemental analyses are inconsistent with the anion formulation of **5**, suggesting that the reaction solution contains multiple products and/or species in equilibrium and that the identity of the isolated solid is thus a function of parameters such as relative solubility; the structural characterization of NR_4^+ or PPh_4^+ salts is currently being sought. The structure of **5a** (*vide infra*) consists of $[Mn_4O_2]$ units (as in **6**) fused or linked together to give a $[Mn_{18}O_{16}]$ core. Thus, **5** may be thought of approximately as an oligomer of **6**, although the mechanism of the formation of **5** is more complicated than implied by this statement, undoubtedly involving fragmentation of **6** and complicated reassembly steps. It is interesting to note that almost all high-nuclearity manganese carboxylate aggregates may be described as approximate oligomers of the basic $[Mn_4O_2]$ unit, providing some elementary level of rationalization, if not prediction, of the identity of products in this area.

Description of Structure. Atomic coordinates for complex **5a** are listed in Table 2, and selected interatomic distances and angles are collected in Tables 3 and 4, respectively. Full details are available in the supplementary material. A labeled ORTEP plot and stereoviews are provided in Figures 1 and 2. The complex crystallizes in monoclinic space group *C2/c* and lies on the crystallographic C_2 axis, which passes through O(14), Mn(4), O(12), O(17), Mn(8), and O(19). The asymmetric unit thus contains half the molecule and five MeCN groups, two ligated to K^+ ions and the other three in the lattice.

The complex comprises eighteen Mn^{III} ions held together by sixteen μ_3-O^{2-} ions to give a $[Mn_{18}O_{16}]^{22+}$ core, with peripheral ligation provided by bridging $PhCO_2^-$ and $phth^{2-}$ groups and

(36) Jiang, Z.-H.; Ma, S.-L.; Liao, D.-Z.; Yan, S.-P.; Wang, G.-L.; Yao, X.-K.; Wang, R.-J. *J. Chem. Soc., Chem. Commun.* **1993**, 745.

Table 3. Selected Interatomic Distances (Å) for $K_4[Mn_{18}O_{16}(O_2CPh)_{22}(phth)_2(H_2O)_4]\cdot 10MeCN$ (**5a**)

Mn(1)···Mn(1′)	2.885(1)	Mn(4)···Mn(5)	2.929(2)
Mn(1)···Mn(2)	2.905(1)	Mn(5)···Mn(6)	3.151(2)
Mn(1)···Mn(3)	3.410(2)	Mn(5)···Mn(6′)	3.186(2)
Mn(1)···Mn(7)	3.428(2)	Mn(6)···Mn(6′)	2.740(2)
Mn(1)···Mn(8)	3.466(2)	Mn(7)···Mn(9)	3.373(2)
Mn(1)···Mn(4)	3.478(2)	Mn(8)···Mn(9)	2.928(2)
Mn(2)···Mn(3)	3.258(2)	Mn(9)···Mn(10′)	3.148(2)
Mn(2)···Mn(7)	3.279(2)	Mn(9)···Mn(10)	3.176(2)
Mn(3)···Mn(5)	3.372(2)	Mn(10)···Mn(10′)	2.764(2)
Mn(1)−O(11)	1.930(4)	Mn(5)−O(69)	2.402(5)
Mn(1)−O(12)	1.929(4)	Mn(6)−O(15′)	1.881(5)
Mn(1)−O(16)	1.928(4)	Mn(6)−O(15)	1.900(5)
Mn(1)−O(17)	1.919(4)	Mn(6)−O(62)	1.929(5)
Mn(1)−O(21)	2.330(5)	Mn(6)−O(71)	1.974(6)
Mn(1)−O(31)	2.331(5)	Mn(6)−O(78)	2.092(5)
Mn(2)−O(11)	1.884(4)	Mn(7)−O(16)	1.905(4)
Mn(2)−O(16)	1.886(4)	Mn(7)−O(18)	1.854(5)
Mn(2)−O(33)	1.986(5)	Mn(7)−O(32)	2.122(5)
Mn(2)−O(42)	2.217(5)	Mn(7)−O(86)	2.257(5)
Mn(2)−O(84)	1.973(5)	Mn(7)−O(95)	1.970(5)
Mn(2)−O(93)	2.188(5)	Mn(7)−O(102)	1.977(5)
Mn(3)−O(11)	1.887(4)	Mn(8)−O(17)	1.885(6)
Mn(3)−O(13)	1.887(5)	Mn(8)−O(18)	2.003(5)
Mn(3)−O(23)	2.131(5)	Mn(8)−O(19)	1.855(6)
Mn(3)−O(35)	2.229(5)	Mn(8)−O(136)	2.296(5)
Mn(3)−O(44)	1.975(5)	Mn(9)−O(18)	1.909(4)
Mn(3)−O(51)	1.955(5)	Mn(9)−O(19)	1.846(2)
Mn(4)−O(12)	1.884(6)	Mn(9)−O(20)	1.930(4)
Mn(4)−O(13)	1.983(4)	Mn(9)−O(104)	1.945(5)
Mn(4)−O(14)	1.849(6)	Mn(9)−O(111)	2.143(5)
Mn(4)−O(135)	2.308(5)	Mn(9)−O(120)	2.371(6)
Mn(5)−O(13)	1.883(4)	Mn(10)−O(20)	1.889(5)
Mn(5)−O(14)	1.861(2)	Mn(10)−O(20′)	1.909(5)
Mn(5)−O(15)	1.943(5)	Mn(10)−O(113)	1.946(6)
Mn(5)−O(53)	1.956(5)	Mn(10)−O(122)	1.967(5)
Mn(5)−O(60)	2.191(5)	Mn(10)−O(129)	2.078(5)
K(A)−O(135′)	2.627(5)	K(B)−O(136)	2.647(5)
K(A)−O(93)	2.716(5)	K(B)−O(42)	2.719(5)
K(A)−O(11)	2.777(5)	K(B)−O(16)	2.744(5)
K(A)−N(142)	2.798(5)	K(B)−O(111)	2.792(5)
K(A)−O(35)	2.907(5)	K(B)−N(145)	2.792(5)
K(A)−O(60)	2.940(5)	K(B)−O(86)	2.816(5)
K(B)−O(18)	2.930(5)		

[a] K(A) and K(B) are labeled K(137) and K(138), respectively, in the supplementary material.

terminal H_2O molecules. The complex has crystallographic C_2 symmetry, but virtual D_2 symmetry. There is a central, almost linear Mn_4 unit [Mn(1), Mn(1′), Mn(2), and Mn(2′)] and seven Mn atoms above and below this unit. The sixteen μ_3-O^{2-} ions connecting the metal centers separate into four classes: (i) O(15), O(18′), O(20), and O(20′) have distinctly trigonal pyramidal geometry with a sum-of-angles (SOA) of ~316°; (ii) O(11), O(11′), and O(16), O(16′) (SOA ≈ 355′) are also pyramidal but with a more flattened geometry; (iii) O(12), O(17) are planar (SOA ≈ 360°) and very approximately trigonal; and (iv) O(14) and O(19) are planar (SOA ≈ 360°) but with an almost T-shaped geometry [Mn(5)−O(14)−Mn(5′) and Mn(9)−O(19)−Mn(9′) are 151.5(3) and 150.9(4)°, respectively]. The unusual T-shaped geometry appears to be enforced by the low rigidity of the outer portions of the $[Mn_{18}O_{16}]^{22+}$ core. The resultant $[Mn_{18}O_{16}]$ structural unit is approximately planar or sheetlike as emphasized by the view in Figure 2 that is approximately along the central Mn_4 axis. As can be seen, the sheetlike core experiences a helical twist about the vertical C_2 axis; this might be due to the presence of the four intimately-associated K^+ ions (*vide infra*), but the K^+-free version would be required to address this point further. The $PhCO_2^-$ groups all bridge only two Mn^{III} ions and are in their familiar *syn,syn*-binding modes, and there are two H_2O molecules on each of the Mn ions Mn(4) and Mn(8).

The two $phth^{2-}$ groups each bridge a total of four Mn atoms with each of their O atoms terminally ligated. This represents a new binding mode for the $phth^{2-}$ group; in $[Mn_4(phth)_2(bpy)_4]^{4+}$, the $phth^{2-}$ groups each bridge three Mn atoms, summarized as follows:

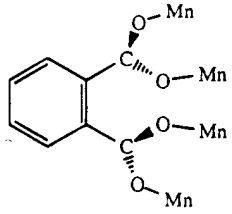

μ_4-$phth^{2-}$

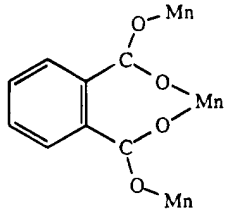

μ_3-$phth^{2-}$

The four K^+ ions are tightly ion-paired with the tetra-anion, and their positions are indicated in Figure 1. Atom K(A) is six coordinate, five of its ligands being O^{2-}, $PhCO_2^-$, and H_2O groups and the sixth being an MeCN (not shown). Atom K(B) is similarly coordinated but is seven coordinate from an additional K···O^{2-} interaction. The present complex thus provides rare examples of K^+···MeCN interactions in the solid state.[37] The intimate association of the K^+ ions with the $Mn_{18}O_{16}$ core makes an alternative description of the complex as a mixed-metal molecular species quite acceptable. Conductivity studies in CH_2Cl_2 indicate a nonelectrolyte, as might be expected in this solvent. The complex is not soluble in MeCN. In DMF and DMSO solution there is evidence that the Mn_{18} core is transformed, and this is under further investigation.

In view of the magnetochemical discussions to be presented below (*vide infra*), it is of interest and beneficial to consider an alternate description of the structure of complex **5a**. The structure can be described as arising from the fusion or linkage of five $[Mn_4(\mu_3\text{-}O)_2]^{8+}$ units possessing either a planar or bent ("butterfly") Mn_4 unit, the latter as found in the parent complex **6**. Fusion of three such units yields the central $[Mn_{10}O_6]$ unit (**I**). The $[Mn_4O_2]$ butterfly units are fused together at "body"

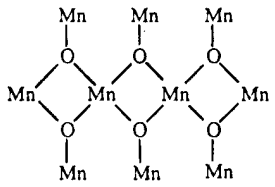

$[Mn_{10}O_6]$
(I)

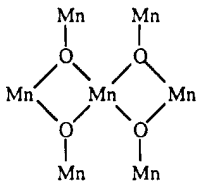

$[Mn_7O_4]$
(II)

(or "hinge") positions, *i.e.*, Mn(1) and Mn(1′). The $[Mn_{10}O_6]$ unit (**I**) is related to the $[Mn_7O_4]$ unit (**II**) previously seen in $[Mn_9Na_2O_7(O_2CPh)_{15}(MeCN)_2]$,[33] $[Mn_9O_7(O_2CPh)_{15}(py)_2]$,[38] and $(NBu^n_4)[Mn_8O_6Cl_6(O_2CPh)_7(H_2O)_2]$ [33] and involves the fusing of *two* $[Mn_4O_2]$ units at a body Mn atom. The $[Mn_{18}O_{16}]$ core of complex **5a** is then completed by the attachment of two additional $[Mn_4O_2]$ units to the $[Mn_{10}O_6]$ subcore at the six "wing-tip" positions *via* the intermediacy of O^{2-} ions O(13), O(13′), O(14), O(18), O(18′), and O(19). As a result of the latter, the two $[Mn_4O_2]$ units at the two ends of the molecule have an O^{2-} ion bridging the two wing-tip Mn atoms [*i.e.*, O(19)

(37) Reiss, C. A.; Goubitz, K.; Heijdenrijk, D. *Acta Crystallogr. Sect. C* **1990**, *C46*, 1084.
(38) Low, D. W.; Eichhorn, D. M.; Draganescu, A.; Armstrong, W. H. *Inorg. Chem.* **1991**, *30*, 877.

Table 4. Selected Bond Angles (deg) for $K_4[Mn_{18}O_{16}(O_2CPh)_{22}(phth)_2(H_2O)_4]\cdot 10MeCN$ (**5a**)

O(11)−Mn(1)−O(12)	99.08(18)	O(71)−Mn(6)−O(78)	89.91(23)	O(13)−Mn(3)−O(35)	171.95(18)	O(104)−Mn(9)−O(111)	92.62(21)
O(11)−Mn(1)−O(16)	79.64(18)	O(16)−Mn(7)−O(18)	88.32(20)	O(23)−Mn(3)−O(44)	85.02(18)	O(104)−Mn(9)−O(120)	86.11(20)
O(11)−Mn(1)−O(17)	171.79(15)	O(16)−Mn(7)−O(32)	98.36(18)	O(23)−Mn(3)−O(51)	89.59(19)	O(111)−Mn(9)−O(120)	172.45(18)
O(11)−Mn(1)−O(21)	86.38(18)	O(16)−Mn(7)−O(86)	85.78(19)	O(35)−Mn(3)−O(44)	89.03(19)	O(20′)−Mn(10)−O(20)	82.50(24)
O(11)−Mn(1)−O(31)	92.78(17)	O(16)−Mn(7)−O(95)	97.38(20)	O(35)−Mn(3)−O(51)	84.16(19)	O(20)−Mn(10)−O(113)	92.80(23)
O(12)−Mn(1)−O(16)	171.93(15)	O(16)−Mn(7)−O(102)	170.26(20)	O(44)−Mn(3)−O(51)	81.42(20)	O(20′)−Mn(10)−O(113)	165.35(21)
O(12)−Mn(1)−O(17)	82.89(19)	O(18)−Mn(7)−O(32)	92.32(19)	O(12)−Mn(4)−O(13)	102.53(13)	O(20)−Mn(10)−O(122)	172.97(21)
O(12)−Mn(1)−O(21)	95.21(12)	O(18)−Mn(7)−O(86)	94.49(19)	O(12)−Mn(4)−O(135)	92.95(11)	O(20′)−Mn(10)−O(122)	94.27(23)
O(12)−Mn(1)−O(31)	85.72(11)	O(18)−Mn(7)−O(95)	174.21(21)	O(13)−Mn(4)−O(13′)	154.95(26)	O(20)−Mn(10)−O(129)	97.32(21)
O(16)−Mn(1)−O(17)	99.51(19)	O(18)−Mn(7)−O(102)	92.99(19)	O(13)−Mn(4)−O(14)	77.47(13)	O(20′)−Mn(10)−O(129)	93.63(23)
O(16)−Mn(1)−O(21)	92.67(18)	O(32)−Mn(7)−O(86)	172.12(19)	O(13)−Mn(4)−O(135)	87.65(17)	O(113)−Mn(10)−O(122)	88.79(23)
O(16)−Mn(1)−O(31)	86.39(17)	O(32)−Mn(7)−O(95)	85.91(18)	O(13)−Mn(4)−O(135′)	91.07(17)	O(113)−Mn(10)−O(129)	100.75(24)
O(17)−Mn(1)−O(21)	85.50(12)	O(32)−Mn(7)−O(102)	91.20(19)	O(13′)−Mn(4)−O(135′)	87.65(17)	O(122)−Mn(10)−O(129)	89.11(21)
O(17)−Mn(1)−O(31)	95.32(11)	O(86)−Mn(7)−O(95)	86.93(18)	O(14)−Mn(4)−O(135)	87.05(11)	Mn(1)−O(11)−Mn(2)	99.23(20)
O(21)−Mn(1)−O(31)	178.83(16)	O(86)−Mn(7)−O(102)	84.50(19)	O(135)−Mn(4)−O(135′)	174.10(22)	Mn(1)−O(11)−Mn(3)	126.57(24)
O(11)−Mn(2)−O(16)	81.91(19)	O(95)−Mn(7)−O(102)	81.55(19)	O(13)−Mn(5)−O(14)	79.73(22)	Mn(2)−O(11)−Mn(3)	119.56(23)
O(11)−Mn(2)−O(33)	96.38(20)	O(17)−Mn(8)−O(18)	102.06(13)	O(13)−Mn(5)−O(15)	167.03(20)	Mn(1′)−O(12)−Mn(1)	96.78(26)
O(11)−Mn(2)−O(42)	95.83(19)	O(17)−Mn(8)−O(19)	179.98 (13)	O(13)−Mn(5)−O(53)	100.61(20)	Mn(1)−O(12)−Mn(4)	131.61(13)
O(11)−Mn(2)−O(84)	179.67(21)	O(17)−Mn(8)−O(136)	92.61(11)	O(13)−Mn(5)−O(60)	92.35(18)	Mn(3)−O(13)−Mn(4)	129.82(23)
O(11)−Mn(2)−O(93)	93.73(19)	O(18′)−Mn(8)−O(18)	155.88(26)	O(13)−Mn(5)−O(69)	98.32(18)	Mn(3)−O(13)−Mn(5)	126.82(23)
O(16)−Mn(2)−O(33)	177.30(20)	O(18)−Mn(8)−O(19)	77.94(13)	O(14)−Mn(5)−O(15)	87.82(23)	Mn(4)−O(13)−Mn(5)	98.45(20)
O(16)−Mn(2)−O(42)	93.14(19)	O(18)−Mn(8)−O(136)	91.30(18)	O(14)−Mn(5)−O(53)	165.65(15)	Mn(4)−O(14)−Mn(5)	104.26(17)
O(16)−Mn(2)−O(84)	98.13(20)	O(18′)−Mn(8)−O(136)	87.61(18)	O(14)−Mn(5)−O(60)	102.23(14)	Mn(5′)−O(14)−Mn(5)	151.5(3)
O(16)−Mn(2)−O(93)	95.19(19)	O(18′)−Mn(8)−O(136′)	91.30(18)	O(14)−Mn(5)−O(69)	82.82(13)	Mn(5)−O(15)−Mn(6)	110.12(22)
O(33)−Mn(2)−O(42)	89.10(19)	O(19)−Mn(8)−O(136)	87.39(11)	O(15)−Mn(5)−O(53)	92.36(20)	Mn(5′)−O(15)−Mn(6)	112.85(23)
O(33)−Mn(2)−O(84)	83.57(20)	O(136′)−Mn(8)−O(136)	174.77(22)	O(15)−Mn(5)−O(60)	86.72(19)	Mn(6′)−O(15)−Mn(6)	92.86(23)
O(33)−Mn(2)−O(93)	82.82(19)	O(18)−Mn(9)−O(19)	80.60(23)	O(15)−Mn(5)−O(69)	83.58(18)	Mn(1)−O(16)−Mn(2)	99.22(20)
O(42)−Mn(2)−O(84)	84.49(19)	O(18)−Mn(9)−O(20)	168.77(21)	O(53)−Mn(5)−O(60)	92.10(20)	Mn(1)−O(16)−Mn(7)	126.82(24)
O(42)−Mn(2)−O(93)	168.11(17)	O(18)−Mn(9)−O(104)	99.26(20)	O(53)−Mn(5)−O(69)	82.94(19)	Mn(2)−O(16)−Mn(7)	119.71(23)
O(84)−Mn(2)−O(93)	85.94(19)	O(18)−Mn(9)−O(111)	90.67(20)	O(60)−Mn(5)−O(69)	168.90(17)	Mn(1′)−O(17)−Mn(1)	97.43(27)
O(11)−Mn(3)−O(13)	88.99(19)	O(18)−Mn(9)−O(120)	96.88(19)	O(15′)−Mn(6)−O(15)	83.14(23)	Mn(1)−O(17)−Mn(8)	131.28(14)
O(11)−Mn(3)−O(23)	99.07(19)	O(19)−Mn(9)−O(20)	88.47(24)	O(15)−Mn(6)−O(62)	166.12(20)	Mn(7)−O(18)−Mn(8)	131.12(24)
O(11)−Mn(3)−O(35)	87.03(18)	O(19)−Mn(9)−O(104)	168.84(17)	O(15′)−Mn(6)−O(62)	92.80(22)	Mn(7)−O(18)−Mn(9)	127.34(24)
O(11)−Mn(3)−O(44)	97.25(20)	O(19)−Mn(9)−O(111)	98.54(14)	O(15)−Mn(6)−O(71)	93.43(22)	Mn(8)−O(18)−Mn(9)	96.86(21)
O(11)−Mn(3)−O(51)	171.11(20)	O(19)−Mn(9)−O(120)	82.85(14)	O(15′)−Mn(6)−O(71)	174.20(22)	Mn(8)−O(19)−Mn(9)	104.57(19)
O(13)−Mn(3)−O(23)	92.47(18)	O(20)−Mn(9)−O(104)	91.96(21)	O(15)−Mn(6)−O(78)	96.37(21)	Mn(9′)−O(19)−Mn(9)	150.9(4)
O(13)−Mn(3)−O(35)	92.88(18)	O(20)−Mn(9)−O(111)	88.40(20)	O(15′)−Mn(6)−O(78)	95.10(22)	Mn(9)−O(20)−Mn(10)	112.50(23)
O(13)−Mn(3)−O(44)	173.56(20)	O(20)−Mn(9)−O(120)	84.22(20)	O(62)−Mn(6)−O(71)	89..44(22)	Mn(9)−O(20)−Mn(10′)	110.17(24)
O(13)−Mn(3)−O(51)	92.65(19)			O(62)−Mn(6)−O(78)	97.21(22)	Mn(10′)−O(20)−Mn(10)	93.40(23)

bridging Mn(9)/Mn(9′) and O(14) bridging Mn(5)/Mn(5′)], shown in structure **III**. This interesting structural unit has not

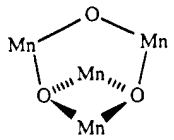

$[Mn_4O_3]$
(III)

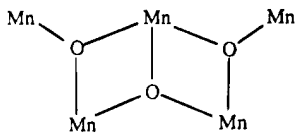

$[Mn_5O_3]$
(IV)

been detected as yet in a discrete tetranuclear complex. Neither have the $[Mn_5O_3]$ unit (**IV**) nor the planar $[Mn_4O_6]$ unit (**V**) at

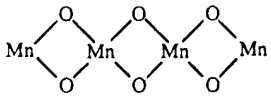

$[Mn_4O_6]$
(V)

the center of the molecule been observed in discrete form; this is unfortunate because it would be particularly desirable to assess the magnitude of the exchange interactions within these discrete units and the resultant spin of their ground states.

Finally, fourteen of the eighteen Mn^{III} ions are six coordinate with distorted-octahedral geometry and exhibit the Jahn−Teller (JT) axial distortion expected for high-spin d^4 ions in near-octahedral geometry; as is almost always the case for Mn^{III}, the JT distortion is an axial elongation where the axially-elongated Mn−O bonds [2.131(5)−2.402(5) Å] are significantly longer than equatorial Mn−O bonds [1.846(2)−1.986(5) Å]. In contrast, Mn(6), Mn(6′), Mn(10), and Mn(10′) are five coordinate with approximately square pyramidal geometry and axial Mn−O bonds (2.078(5) and 2.092(5) Å) noticeably longer than the basal Mn−O bonds [1.88(5)−1.974(5) Å].

Magnetochemistry of Complex 5. Magnetic susceptibility experiments were carried out on a solid sample of complex **5a** dried under vacuum. Under these conditions all of the MeCN solvate molecules are lost (*i.e.*, complex **5**). Variable-temperature dc magnetic susceptibility studies were performed on a parafilm-restrained powdered sample of complex **5** in the temperature range 2.00−320 K and in an applied magnetic field of 10 kG. As can be seen in Figure 3, $\chi_M T$ slowly decreases from 28.7 cm^3 K mol^{-1} (15.1 μ_B/molecule) at 320 K to 0.376 cm^3 K mol^{-1} (1.73 μ_B) at 2.00 K, where χ_M is the molar dc magnetic susceptibility per Mn_{18} complex. The spin-only value for an aggregate of eighteen noninteracting Mn^{III} ($S = 2$) ions is 54.0 cm^3 K mol^{-1} (20.8 μ_B). It is clear that there are appreciable antiferromagnetic exchange interactions within complex **5**.

Each Mn^{III} ion in complex **5** has a $2S + 1 = 5$-fold degeneracy, which leads to a 5^{18}-fold degeneracy for the spin states in this Mn^{III}_{18} complex. The total spin of the different spin states of complex **5** ranges from $S = 0$ to $S = 36$. There is a total of approximately 3.8×10^{12} different spin states. Only one state has $S = 36$; there are 17 states with $S = 35$, 153 with $S = 34$, and so on, with the spin ladder terminating with roughly 3.3×10^9 states with a total spin of $S = 0$. With present quantum-mechanical approaches[25] the large number of spin states present in complex **5** makes it a near-to-impossible task to least-squares fit (or even simulate) the $\chi_M T$ *vs* temperature data given in Figure 3. Thus, it is not possible to evaluate the

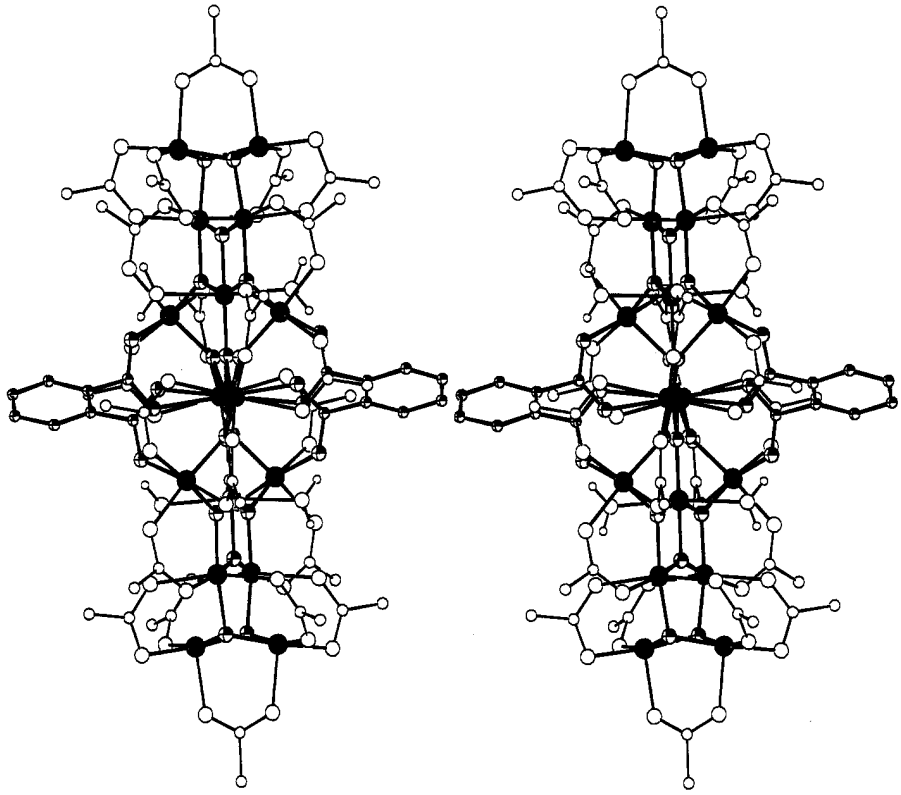

Figure 2. ORTEP stereopair of complex **5a** (without the K^+ ions) from a viewpoint essentially perpendicular to that in Figure 1 and approximately along the almost linear Mn_4 central unit. This view emphasizes the twist of the almost planar $[Mn_{18}O_{16}]$ core along the C_2 (vertical) axis.

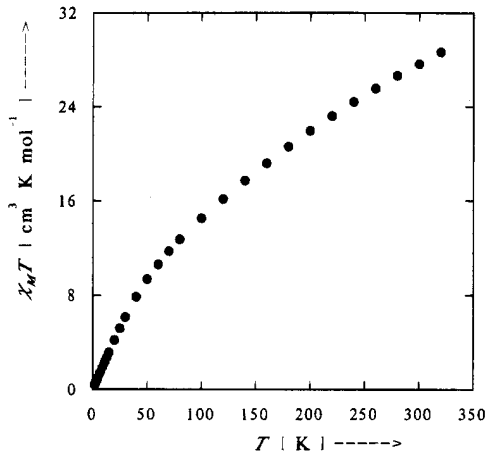

Figure 3. Plot of $\chi_M T$ *vs* temperature data for a polycrystalline sample of $K_4[Mn_{18}O_{16}(O_2CPh)_{22}(phth)_2(H_2O)_4]$ (**5**). χ_M is the molar dc magnetic susceptibility measured in a 10.0 kG field.

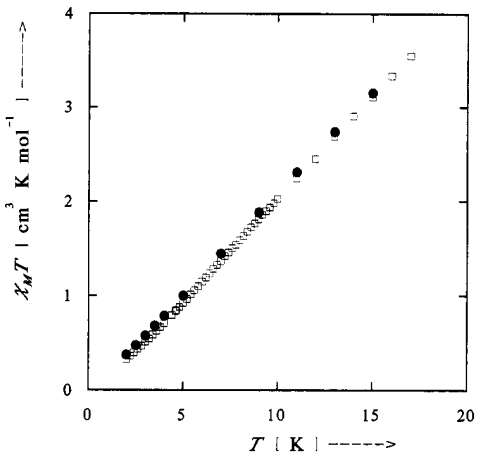

Figure 4. Plot of $\chi_M T$ *vs* temperature data for a polycrystalline sample of $K_4[Mn_{18}O_{16}(O_2CPh)_{22}(phth)_2(H_2O)_4]$ (**5**). Ac magnetic susceptibility data (□) measured in zero dc field with a 1.0 G ac field oscillating at 50 Hz are plotted. The dc data (●) are shown for comparison purposes.

magnetic exchange parameters (J in $\hat{H} = -2J\hat{S}_i \cdot \hat{S}_j$) that characterize the pairwise magnetic exchange interactions in complex **5**.

Magnetization data were collected from 2.0 to 4.0 K for the parafilm-restrained powdered sample at several magnetic fields in the 0.50−50.0 kG range. At the highest field the reduced magnetization, $M/N\mu_B$, where N is the Avogadro number and μ_B is the Bohr magneton, reached a value of 1.63. It was not possible to fit all of the data assuming that only one spin state is occupied in the 2.0−4.0 K range in fields of 0.50−50.0 kG. Even in this narrow temperature range, several different states apparently are thermally populated.

In an effort to determine the spin of the ground state of complex **5**, ac magnetic susceptibility data were also collected for the powder sample in the 2.0−60.0 K range. These data were run in zero dc magnetic field with a 1.0 G magnetic field oscillating at 50 Hz. As can be seen in Figure 4, the ac susceptibility data nearly superimpose on the dc data. Both the dc and the ac plots of $\chi_M T$ *vs* temperature extrapolate to $\chi_M T \simeq 0$ as the temperature goes to zero. It has to be concluded that Mn^{III}_{18} complex **5** has a $S = 0$ ground state. Finally, it should also be noted that no out-of-phase ac magnetic susceptibility signal was seen for complex **5** in the 2.0−60.0 K range.

Origin of $S = 0$ Ground State. There is a growing list of polynuclear manganese complexes with average metal oxidation states greater than or equal to +3. With one exception, the spin of the ground state of these complexes is relatively large. The $[Mn_{12}O_{12}(O_2CR)_{16}(H_2O)_4]$ complexes have a ground state with either $S = 9$ or $S = 10$, depending on the R substituent.[24-26] The one-electron reduction product with a valence-trapped $Mn^{IV}_4Mn^{III}_7Mn^{II}$ structure, *i.e.*, $(PPh_4)[Mn_{12}O_{12}(O_2CEt)_{16}$-

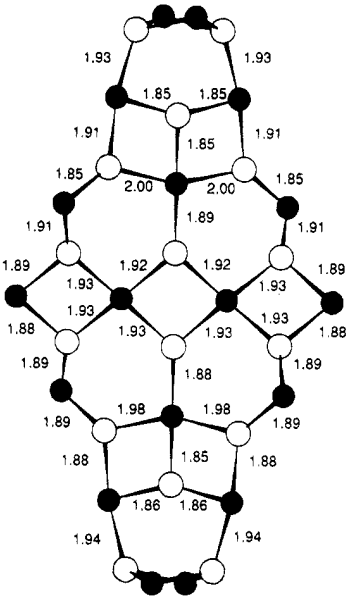

Figure 5. A drawing of the $[Mn_{18}O_{16}]^{22+}$ core of $K_4[Mn_{18}O_{16}(O_2CPh)_{22}(phth)_2(H_2O)_4]$ (**5**). Mn−O bond lengths (Å) are given for all bridging μ_3-O^{2-} ions. The manganese atoms are shaded.

$(H_2O)_4]$, has a $S = {}^{19}/_2$ ground state.[26] The two structurally related Mn^{III}_x complexes $[Mn_9Na_2O_7(O_2CPh)_{15}(MeCN)_2]$ and $(NBu^n_4)[Mn_8O_6Cl_6(O_2CPh)_7(H_2O)_2]$ have been found[20b] to have $S = 4$ and $S = 11$ ground states, respectively. $[Mn_{10}O_8(O_2CPh)_6(pic)_8]$ (picH is picolinic acid) is the one known polynuclear Mn^{III} complex that does not have a relatively high-spin ground state. Preliminary data for this Mn^{III}_{10} complex point to a $S = 0$ ground state.[22a] Thus, for the present Mn^{III}_{18} complex **5** it is important to rationalize the $S = 0$ ground state.

As indicated above, complex **5** can be described as arising from the fusion or linkage of five $[Mn_4(\mu_3\text{-}O)_2]^{8+}$ butterfly units. Three such butterfly units are fused at a body Mn atom to give **I**. It has been established that spin frustration is present in $[Mn_4O_2]^{8+}$ butterfly complexes where both the body−body and the wing-tip−body magnetic exchange interactions are antiferromagnetic. The body−body antiferromagnetic interaction is greater than the wing-tip−body interaction. This causes spin frustration. The spins on the two body Mn^{III} ions are almost paired up. Each wing-tip Mn^{III} ion interacts with both of the body Mn^{III} ions and would align its spin antiparallel to both if possible, but cannot do so. The resultant spin alignment in such a Mn^{III}_4 butterfly complex is as follows:

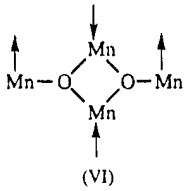

(VI)

All known $[Mn_4O_2]^{8+}$ butterfly complexes have a $S = 3$ ground state. Thus, the spins on the two body Mn^{III} ions are not totally paired up, but pair to give a resultant spin operator of $\hat{S}_{bb} = 1$. The spins ($S = 2$) on each of the two wing-tip ions are frustrated and maintain a mutually parallel alignment such that most of the unpaired spin density resides on the wing-tip ions in the $S = 3$ ground state.

In Figure 5 is shown a drawing of the $[Mn_{18}O_{16}]^{22+}$ core of complex **5**. All of the eighteen Mn^{III} ions are interconnected by μ_3-O^{2-} ions. The bond lengths of all of the Mn−O bonds in the $[Mn_{18}O_{16}]^{22+}$ core are given in Figure 5 and fall in the 1.85−1.98 Å range. At the center of complex **5** are three body-fused butterfly complexes. It would be expected that the body−body exchange interactions in each of the three fused butterfly units would dominate the wing-tip−body interactions and this would give a spin alignment that would look approximately as follows:

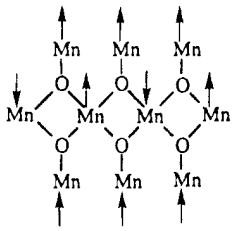

(VII)

There would probably not be a total pairing of spins on the four central body ions. If the degree of spin frustration in **VII** was exactly the same as that found for $[Mn_4O_2]^{8+}$ butterfly complexes, then the ground state of the **VII** unit would be expected to be $S = 10$ with most of the unpaired spin residing on the six wing-tip ions. This estimate of a S value for the **VII** moiety is probably too high, for there are antiferromagnetic exchange interactions present between pairs of wing-tip Mn^{III} ions.

To complete the $[Mn_{18}O_{16}]^{22+}$ core of complex **5** two additional $[Mn_4O_2]^{8+}$ butterfly units are attached via three μ_3-O^{2-} ions, each to the central unit **VII**. Each of the wing-tip ions of these last two butterfly units also serve as body ions in a butterfly unit that develops as a result of the attachment. Thus, it would be reasonable to expect the spin orientation on the wing-tip ions of the last two butterflies to be antiparallel to that on the wing-tip ions of the **VII** unit. The net result would be that the $S \simeq 3$ spin of each of the last two attached butterflies would be antiparallel to the $S \leq 10$ spin of the central $[Mn_{10}O_6]^{18+}$ unit (**VII**). The overall approximate spin alignment would be as follows:

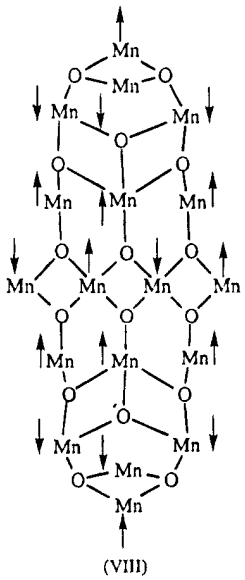

(VIII)

As drawn in the preceding structure, the spin alignment on ten of the Mn^{III} ions are parallel, but antiparallel to the spin

orientation on the other eight Mn^{III} ions. If the spin on the central $[Mn_{10}O_6]^{18+}$ core is $S \leq 10$, and each of the last two butterflies that are attached have a $S = 3$ spin that is antiparallel, this would give a total spin for complex **5** of $S \leq 4$. In this way it is possible to anticipate that the ground state spin of complex **5** would be low.

Acknowledgment. This work was supported by NSF Grants CHE-9115286 (D.N.H.), CHE-9420322 (D.N.H.), and CHE-9311904 (G.C.) and NIH Grants GM39083 (G.C.) and HL13652 (D.N.H.). The ac magnetic susceptibility measurements were performed with an ac SQUID susceptometer in the Center for Interface and Materials Science (UCSD) which was funded by the W. A. Keck Foundation.

Supporting Information Available: Text summarizing the data collection and tables listing crystallography data for complex **5**, including program MU output (Table S1), crystal and diffractometer data (Table S2), fractional coordinates (Table S3), anisotropic thermal parameters (Table S4), bonded distances and angles (Table S5), standard data tape (Table S6), Mn−Mn distances and angles to 3.5 Å (Table S7), K^+-coordination to 3.0 Å (Table S8), and hydrogen bonding parameters (Table S9) (45 pages). Ordering information is given on any current masthead page.

IC950209R